Fine-Tuning Nanoparticle Packing at Water−Oil Interfaces Using Ionic Strength

Yu Chai,[†,‡,||] Alysia Lukito,[§] Yufeng Jiang,[||] Paul D. Ashby,*,[‡] and Thomas P. Russell*,[†,⊥,#]

[†]Materials Sciences Division and [‡]Molecular Foundry, Lawrence Berkeley National Laboratory, 1 Cyclotron Road, Berkeley, California 94720, United States

[§]Department of Chemical and Biomolecular Engineering and [||]Department of Materials Science and Engineering, University of California, Berkeley, Berkeley, California 94720, United States

[⊥]Polymer Science and Engineering Department, University of Massachusetts Amherst, Amherst, Massachusetts 01003, United States

[#]Beijing Advanced Innovation Center for Soft Matter, Science and Engineering, Beijing University of Chemical Technology, Beijing 100029, China

Ⓢ *Supporting Information*

ABSTRACT: Nanoparticle-surfactants (NPSs) assembled at water−oil interfaces can significantly lower the interfacial tension and can be used to stabilize liquids. Knowing the formation and assembly and actively tuning the packing of these NPSs is of significant fundamental interest for the interfacial behavior of nanoparticles and of interest for water purification, drug encapsulation, enhanced oil recovery, and innovative energy transduction applications. Here, we demonstrate by means of interfacial tension measurements the high ionic strength helps the adsorption of NPSs to the water−oil interface leading to a denser packing of NPSs at the interface. With the reduction of interfacial area, the phase transitions from a "gas"-like to "liquid" to "solid" states of NPSs in two dimensions are observed. Finally, we provide the first *in situ* real-space imaging of NPSs at the water−oil interface by atomic force microcopy.

KEYWORDS: *Nanoparticles, liquid−liquid interfaces, in situ AFM, self-assembly, surfactants, interfacial tension*
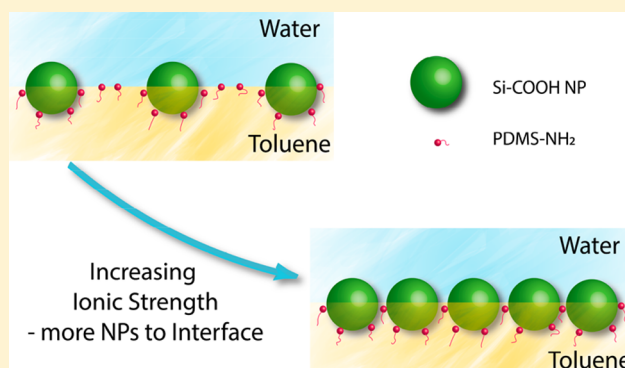
Emulsions stabilized by the interfacial segregation of solid, colloidal particles are called Pickering emulsions.[1−4] Pickering emulsions are more stable than classic surfactant stabilized emulsions due to the significant reduction in interfacial energy by each solid particle that irreversibly binds to the interface. Pickering emulsions have found widespread uses, including solid phase extraction,[5,6] drug encapsulation,[7] and enhanced oil recovery.[8,9] Depending on the uniformity of their size, the colloidal particles confined to the interface can densely pack into 2D crystalline arrays as the emulsions coarsen, reducing the interfacial energy.[10] An alternate strategy is to disperse functionalized nanoparticles (NPs) in one fluid and ligands, oligomeric or polymeric, in the second immiscible fluid, that are end-functionalized where the functionalization is complementary to the functionality on the NPs.[11,12] The NPs and the ligands will interact at the interface, forming nanoparticle surfactants (NPSs) that act as surfactants, reducing the interfacial energy. The NPSs form at the interface and assemble into a monolayer, maximizing the reduction in the interfacial tension. This latter approach is far simpler than using colloidal particles, since with colloidal particles the surface chemistry of the colloidal particles must be carefully tuned to

ensure the formation of a monolayer at the interface, whereas with NPSs their formation is spontaneous and self-regulated. No special chemistries are necessary. If the fluid phases are perturbed by use of an external field (shear or electric field, for example), the interfacial area will increase, more NPSs will form and assemble at the interface and upon release of the external field the interfacial area will decrease, compressing the assembly of NPSs and ultimately causing the NPS assembly to jam, prohibiting any further change at the interface. In so doing, highly nonequilibrium shapes of the fluids can be locked in, forming what is termed as a structured liquid.[11] The jamming of the NPS' assemblies and the structuring of two immiscible liquids has potential use in encapsulation and delivery, since the ligands on the NPs can be made responsive to chemical triggers,[13] for the generation of bicontinuous interfacially jammed emulsions or bijels, for generating solid systems with pathways for charge or ion transduction comparable to that of a

pure liquid,[14] or for three-dimensional (3D) printing of one fluid phase in a second fluid.

In the case of silica NPs functionalized with carboxylic acid groups that are dispersed in water and polymer chains end-functionalized with an amine group, the system used in this work, the electrostatic interactions of these components at the interface drives the formation of the NPSs. While the electrostatic attractions between the NPs and surfactants anchor the NPSs to the interface, the electrostatic interactions between the NPs hinder the adsorption of NPs to the interface. Consequently, controlling the electrostatic interactions affords a route to precisely control the formation and assembly of the NPSs. It is known that ionic strength can dramatically affect the electrostatic forces in solution[15−17] and, therefore, NPS formation as well. Here, we systematically investigated the manner in which ionic strength could be used to actively manipulate the packing of the NPSs at the interface, as indicated in the cartoon in Figure 1. Interfacial tension
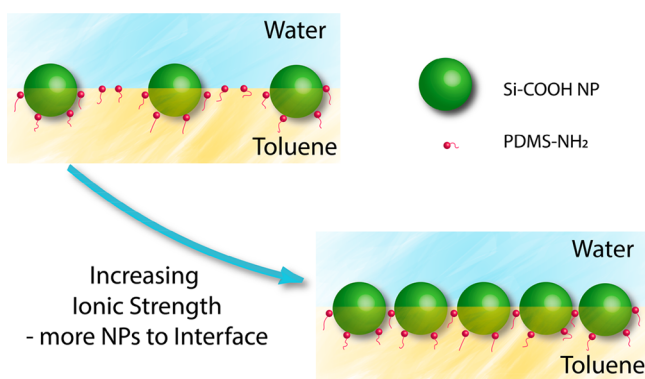

Figure 1. Schematic diagram of the NP-surfactants assembled at the water−toluene interface at different ionic strength conditions.

measurements serve as a convenient means to quantify the assembly, since the lower the interfacial tension, the greater will be the number of NPSs formed at the interface. Atomic force microscopy (AFM) was used to image the jammed assembly of the NPSs at the interface.

All samples were made from commercial chemicals, where carboxylated silica nanoparticles (original concentration of 2.5 w/w%) with a diameter of 13 nm (Figure S3) were purchased from Microspheres-Nanospheres, monoamine terminated polydimethylsiloxane (M_w = 2000 g/mol) from Gelest, and sodium chloride (NaCl, purity >99.999%) from Sigma-Aldrich. The concentration of NP-COOH and PDMS-NH$_2$ used in this study were 1 mg/mL and 1 w/w%, respectively. The 1 mg/mL NP-COOH solutions with different ionic strengths were made by diluting the as-received bulk NP-COOH solution with the concentrated NaCl solution and pure water, where the pH was adjusted with the addition of 1 M hydrogen chloride solution or 1 M sodium hydroxide solution and measured with a Mettler Toledo El20 pH meter. The 1 w/w% PDMS-NH$_2$ was made by dissolving the as-received PDMS-NH$_2$ in toluene without any further treatment. The interfacial tension experiments were performed on a KRUSS tensiometer by the pendent drop method, where the volume of pendent drops was 40 μL. The AFM measurements were performed on a Cypher ES AFM (Asylum Research) with BL-AC40TS tips (Olympus). Instead of using 1 w/w% PDMS-NH$_2$ toluene solution, the AFM experiments used the same concentration of PDMS-NH$_2$

solution but dissolved in a viscous silicone oil (Sigma-Aldrich, viscosity = 60,000 cSt).

Without NP-surfactants, the interfacial tension is 35 mN/m (Figure S1), which is consistent with the literature.[18] With the functionalized NPs dispersed in the water and amine-terminated polymer dissolved in the toluene, the formation and assembly of the NPSs at the interface causes a very rapid initial reduction in the interfacial tension, followed by a further gradual decrease in the interfacial tension. As the concentration of NaCl in the aqueous phase is increased, a consistent decrease in the interfacial tension is observed when NPSs are formed. This result indicates that the areal density of NPSs at the toluene−water interface increases with increasing ionic strength or NaCl concentration in the aqueous phase. If we take the interfacial tension after 1 h of incubation time as being a quasi-equilibrium interfacial tension, the reduction in the interfacial tension is evident (Figure 2). Initially, the interfacial tension
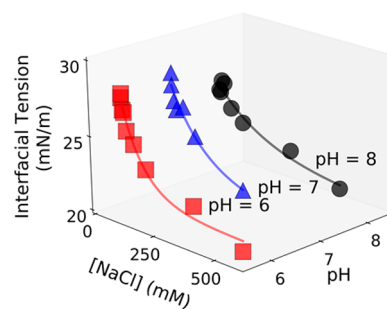
Figure 2. Interfacial tension after 1 h of aging as a function of NaCl concentration at a pH of 6, 7, and 8.

decreases rapidly with salt addition and then begins to saturate for salt concentrations >300 mM. As the pH of the aqueous phase is increased, the reduction in the interfacial tension is less rapid initially, but for salt concentrations >300 mM the interfacial tension is seen to be independent of pH.

After aging, the interface of the droplet is covered by a uniform monolayer of NPS. If the aqueous phase is withdrawn from the droplet, the interfacial area decreases, the areal density of the NP-surfactants at the interface increases causing the interfacial tension to decrease.[19−21] If the volume of the droplet is decreased at a constant rate of 40 μL/min, the interfacial area decreases at a constant rate or, in other words, the assembly of the NPSs at the interface is compressed at a constant rate. Shown in Figure 3a is the interfacial tension as a function of inverse surface area at different concentrations of salt, where all interfacial tension data were cut off at the point where visible wrinkles, that is, where the NPS assembly jams or vitrifies into an elastic layer at the interface. At this point, the Young−Laplace equation is no longer valid. As the salt concentration increases, the dynamic interfacial tension curve behaves differently. The first data point of each curve is identical to the values in Figure 2, since the withdrawal of the aqueous phase immediately followed the aging experiments. All of these profiles are similar in shape, suggesting that the results can be shifted horizontally. If we normalize all these data to the surface area of the droplet when wrinkling is first observed, SA$_W$, the results in Figure 3b are obtained. An overlap between the data for all salt concentrations is observed. Two different regimes are evident. One characterized by a gradual decrease in the interfacial tension with decreasing surface area which is followed by a regime where the decrease in the interfacial
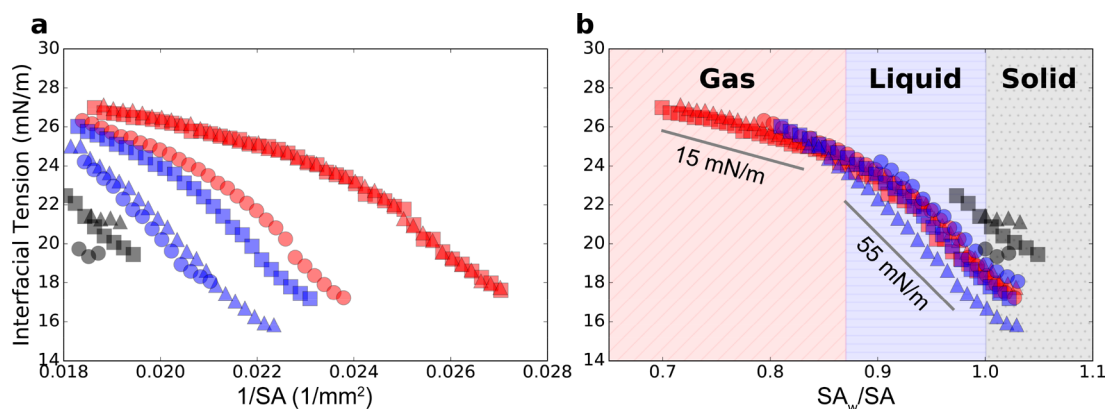
Figure 3. (a) Dynamic interfacial tension of pendent drops of water with 1 mg/mL NP-COOH immersed in toluene with 1 w/w% PDMS-NH$_2$ measured when withdrawing the solution from pendent drops after 1 h of aging at different NaCl concentrations at pH = 6, where the x-axis is inverse surface area. (b) Normalized dynamic interfacial tension, where the shaded areas indicate three phases of the NPSs. The concentrations of NaCl are 0 (red squares), 1 (red triangles), 5 (red circles), 10 (blue squares), 20 (blue triangles), 50 (blue circles), 100 (black squares), 300 (black triangles), and 500 (black circles) mM.

tension is more rapid with decreasing surface area. Finally, there is a kink in the data where for much smaller interfacial areas, the assemblies of NPSs wrinkle (at SA$_w$/SA = 1). For the higher NaCl concentrations (>300 mM), only one regime is observed before the assemblies wrinkle.

The slopes of these curves at any point has a unit of mN/m,[21] which corresponds to the moduli of the interfacial assemblies, and it is evident that outside of the jammed elastic assembly formed at high compression ratios there are two different types of assemblies having distinct moduli that fall into two different regimes of SA$_w$/SA. For small SA$_w$/SA, the NPSs are loosely packed at the interface and the modulus is low (15 mN/m). As SA$_w$/SA increases, the NPSs cannot freely diffuse in the plane of the interface but must rely on a cooperative motion of many NPSs. These types of packing are directly analogous to the different states of molecules seen in Langmuir monolayers[22] where for high surface areas the molecules are packed in a "gas" state, and with decreasing surface area, the monolayer undergoes a phase transition from the "gas" to "liquid" state. In the liquid state, the motions of the NPSs are energetically more costly and as such the modulus increases from 15 to 55 mN/m. It should be noted that the "liquid" state is accessible either by a significant reduction in the interfacial area or by adding more NaCl. This equivalence suggests that a high ionic strength can significantly enhance the adsorption of NPs to the interface and result in a dense packing of NP-surfactants at the interface. For higher compression ratios, the assemblies, as with Langmuir monolayers, undergo a further phase transition from the liquid state into the solid state where the assemblies show elastic behavior and wrinkle. From these results, it is evident that at high salt concentrations the formation and assembly of the NPSs occurs rapidly, along with the transitioning into the "solid" state. In a sense, we can liken this to a solidification from the liquid state (like crystallization) and from the gaseous state (sublimation).

The onset of visible wrinkling defines the point at which the NPS assemblies are densely packed.[23] So, if V_w is the volume where the first visible wrinkle is observed and V_i is the initial volume of the drop, then V_w/V_i defines the amount that the quasi-equilibrium assembly of NPSs must be compressed to solidify the assembly. Figure 4 shows V_w/V_i as a function of the salt concentration after 1 h of aging. V_w/V_i monotonically increases as the salt concentration increases at all measured pHs
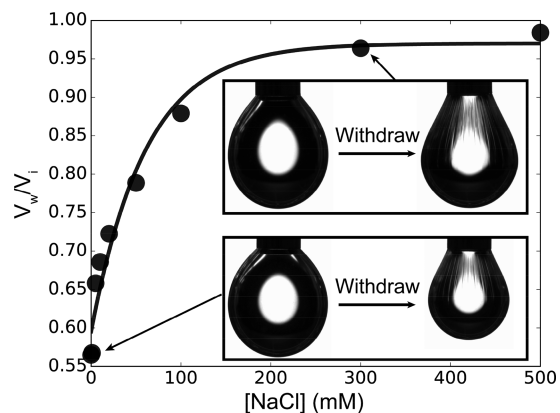

Figure 4. Compression ratio of aged droplets as a function of the NaCl concentration at pH = 6. Images of droplets are snapshots during the withdrawing process at 0 mM and 300 mM NaCl, respectively.

(Figure S2). The insets are snapshots captured during experiments where the aqueous phase was withdrawn from the droplets, where two typical salt concentrations are shown. For each, the image on the left-hand side was taken after 1 h of aging, whereas the image on the right-hand side was taken when visible wrinkles were initially observed. It is evident that at high salt concentrations, visible wrinkling is observed without a significant amount of compression, which is consistent with our argument that the high ionic strength promotes the formation of NPSs and the generation of high areal density NPS assemblies.

In addition to interfacial tension measurements, *in situ* atomic force microscopy (AFM) was performed on the NPSs assembled at the water–oil interface. These noninvasive measurements directly image the NPS assemblies *in situ* at the liquid–liquid interface. Here, the AFM tip was immersed in the water with the dispersed NPs and brought directly into contact with the water–oil interface. Previous measurements[24,25] have been performed on surfactant-decorated NPs (all in water) at the liquid–liquid interface where the oil phase was pure. In our experiment, NPs were dispersed in the water, end-functionalized polymer dissolved in a silicone oil, and the NPSs formed at the interface. Consequently, the AFM probe must be immersed in either the NP dispersion in water or in

the silicone oil solution. This makes the imaging more difficult and to the best of our knowledge this is the first direct AFM imaging under such conditions. The inset in Figure 5 shows the
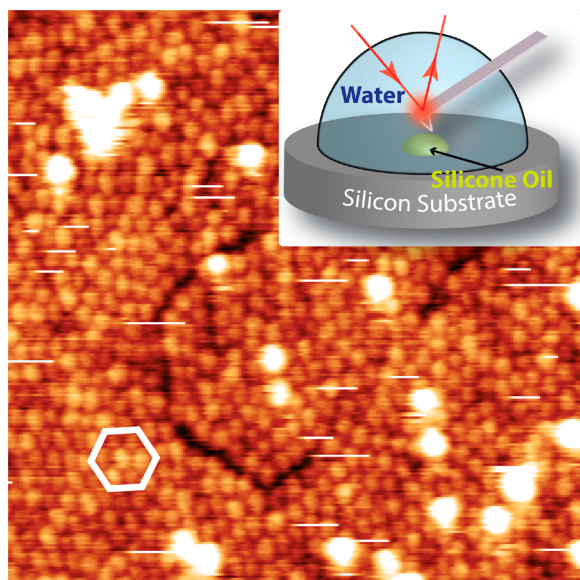
Figure 5. In situ AFM image of the NPs assembled at the water−silicone oil interface at 100 mM NaCl, where the white hexagon shows the hexagonal packing of NPs and the inset shows the schematic diagram of the experimental setup. The image size is 500 nm.

experimental configuration. Before imaging, a small drop of silicon oil (viscosity = 60,000 cSt) with 1 w/w% of PDMS-NH$_2$ was placed on a silicon substrate and a small drop of water with 1 mg/mL NP-COOH was placed on top of the silicone oil to completely cover the oil phase. Then, the sample was placed in a Cypher ES sealed sample cell for at least 1 h to let the NPSs form and assemble at the water−oil interface. While imaging, the AFM probe was immersed in the water bridge formed between the sample and the cantilever holder. Figure 5 shows the in situ AFM image of the interface between the water and silicone oil that is covered by the NPSs with a NaCl concentration of 100 mM. A close packing of the NPSs is observed. The white hexagon indicates a hexagonal packing of the NPSs. It is interesting that the packing of NPSs shows some degree of order, suggesting that there are local areas of the NPSs that form crystalline-like arrays. In addition, a grain boundary is shown in the image indicating that the NPSs might form 2D aggregates at the early stages of the assembly. Repeated imaging of a fixed area showed no observable movement of the NPSs occurred. Hence, the motion of NPSs is arrested, which is consistent with a jammed or glassy assembly. As time elapses, during the aging and experimental setup time, due to solvent evaporation, the interfacial area decreases, and the areal density of the NPSs increases, causing aggregates to coalesce, cover the entire interface, and jam or vitrify. The AFM image shows the microscopic structure of the NPS assemblies characteristic of the shaded area in Figure 3b.

We have demonstrated the use of ionic strength to tune the interfacial packing of NP-surfactants at the water−oil interface. As the ionic strength increases, the adsorption of NP to the liquid interface can be markedly enhanced resulting a dense packing of NPSs. Both the interfacial tension and high-speed image analysis experiments have been conducted to show the relation between the ionic strength and the packing density of

the NPSs at the water−oil interface. Evidence is shown for phase transitions of the assemblies from a "gas"-like state to a "liquid"-like state and then into a densely packed state. In addition, the first in situ AFM images of NPSs at the water−oil interface are shown and provide a real-space view of the packing of the NPSs assembled at the water−oil interface.

■ ASSOCIATED CONTENT

Ⓢ Supporting Information

The Supporting Information is available free of charge on the ACS Publications website at DOI: 10.1021/acs.nano-lett.7b03462.

Time-dependent liquid−liquid interfacial tension at different salt concentrations, compression ratio of aged droplets as a function of the NaCl concentration at different pHs, and size distribution of NPs determined by DLS (PDF)

■ AUTHOR INFORMATION

Corresponding Authors
*E-mail: pdashby@lbl.gov (P.D.A.).
*E-mail: russell@mail.pse.umass.edu (T.P.R.).

ORCID Ⓞ
Thomas P. Russell: 0000-0001-6384-5826

Notes
The authors declare no competing financial interest.

■ REFERENCES

(1) Pickering, S. U. CXCVI.—Emulsions. *J. Chem. Soc., Trans.* **1907**, 91, 2001−2021.
(2) Chevalier, Y.; Bolzinger, M. Colloids and Surfaces A: Physicochemical and Engineering Aspects Emulsions Stabilized with Solid Nanoparticles: Pickering Emulsions. *Colloids Surf., A* **2013**, 439, 23−34.
(3) Levine, S.; Bowen, B. D.; Partridge, S. J. Stabilization of Emulsions by Fine Particles I. Partitioning of Particles between Continuous Phase and Oil/water Interface. *Colloids Surf.* **1989**, 38, 325−343.
(4) Yang, Y.; Fang, Z.; Chen, X.; Zhang, W.; Xie, Y.; Chen, Y.; Liu, Z.; Yuan, W. An Overview of Pickering Emulsions: Solid-Particle Materials, Classification, Morphology, and Applications. *Front. Pharmacol.* **2017**, 8, 1−20.
(5) Augusto, F.; Hantao, L. W.; Mogollón, N. G. S.; Braga, S. C. G. N. New Materials and Trends in Sorbents for Solid-Phase Extraction. *TrAC, Trends Anal. Chem.* **2013**, 43, 14−23.
(6) Yang, J.; Li, Y.; Wang, J.; Sun, X.; Cao, R.; Sun, H. Analytica Chimica Acta Molecularly Imprinted Polymer Microspheres Prepared by Pickering Emulsion Polymerization for Selective Solid-Phase Extraction of Eight Bisphenols from Human Urine Samples. *Anal. Chim. Acta* **2015**, 872, 35−45.
(7) Frelichowska, J.; Bolzinger, M.; Valour, J.; Mouaziz, H.; Pelletier, J.; Chevalier, Y. Pickering W/o Emulsions: Drug Release and Topical Delivery. *Int. J. Pharm.* **2009**, 368, 7−15.
(8) Yoon, K. Y.; Son, H. A.; Choi, S. K.; Kim, J. W.; Sung, W. M.; Kim, H. T. Core Flooding of Complex Nanoscale Colloidal Dispersions for Enhanced Oil Recovery by in Situ Formation of Stable Oil-in-Water Pickering Emulsions. *Energy Fuels* **2016**, 30, 2628−2635.

(9) Shamsijazeyi, H.; Miller, C. A.; Wong, M. S.; Tour, J. M.; Verduzco, R. Polymer-Coated Nanoparticles for Enhanced Oil Recovery. *J. Appl. Polym. Sci.* **2014**, *131*, 1−13.

(10) Li, B.; Zhou, D.; Han, Y. Assembly and Phase Transitions of Colloidal Crystals. *Nat. Rev. Mater.* **2016**, *1*, 15011.

(11) Cui, M.; Emrick, T.; Russell, T. P. Stabilizing Liquid Drops in Nonequilibrium Shapes by the Interfacial Jamming of Nanoparticles. *Science* **2013**, *342*, 460−463.

(12) Feng, T.; Hoagland, D. A.; Russell, T. P. Assembly of Acid-Functionalized Single-Walled Carbon Nanotubes at Oil/water Interfaces. *Langmuir* **2014**, *30*, 1072−1079.

(13) Huang, C.; Sun, Z.; Cui, M.; Liu, F.; Helms, B. A.; Russell, T. P. Structured Liquids with pH-Triggered Reconfigurability. *Adv. Mater.* **2016**, *28*, 6612−6618.

(14) Toor, A.; Helms, B. A.; Russell, T. P. Effect of Nanoparticle Surfactants on the Breakup of Free-Falling Water Jets during Continuous Processing of Reconfigurable Structured Liquid Droplets. *Nano Lett.* **2017**, *17*, 3119−3125.

(15) Ábrahám, Á.; Kardos, A.; Mezei, A.; Campbell, R. A.; Varga, I. Effects of Ionic Strength on the Surface Tension and Nonequilibrium Interfacial Characteristics of Poly(sodium Styrenesulfonate)/ Dodecyltrimethylammonium Bromide Mixtures. *Langmuir* **2014**, *30*, 4970−4979.

(16) Palladino, P.; Ragone, R. Ionic Strength Effects on the Critical Micellar Concentration of Ionic and Nonionic Surfactants: The Binding Model. *Langmuir* **2011**, *27*, 14065−14070.

(17) Dugyala, V. R.; Muthukuru, J. S.; Mani, E.; Basavaraj, M. G. Role of Electrostatic Interactions on the Adsorption Kinetics of Nanoparticles at Fluid-Fluid Interfaces. *Phys. Chem. Chem. Phys.* **2016**, *18*, 5499−5508.

(18) Prokop, R. M.; Hair, M. L.; Neumann, A. W. Interfacial Tension of a Polystyrene−Poly(ethylene Oxide) Diblock Copolymer at the Water−Toluene Interface. *Macromolecules* **1996**, *29*, 5902−5906.

(19) Vatanparast, H.; Javadi, A.; Bahramian, A. Silica Nanoparticles Cationic Surfactants Interaction in Water-Oil System. *Colloids Surf., A* **2017**, *521*, 221−230.

(20) Maestro, A.; Deshmukh, O. S.; Mugele, F.; Langevin, D. Interfacial Assembly of Surfactant-Decorated Nanoparticles: On the Rheological Description of a Colloidal 2D Glass. *Langmuir* **2015**, *31*, 6289−6297.

(21) Maestro, A.; Rio, E.; Drenckhan, W.; Langevin, D.; Salonen, A.; Anniina, S. Foams Stabilised by Mixtures of Nanoparticles and Oppositely Charged Surfactants: Relationship between Bubble Shrinkage and Foam Coarsening. *Soft Matter* **2014**, *10*, 6975−6983.

(22) Santini, E.; Krägel, J.; Ravera, F.; Liggieri, L.; Miller, R. Study of the Monolayer Structure and Wettability Properties of Silica Nanoparticles and CTAB Using the Langmuir Trough Technique. *Colloids Surf., A* **2011**, *382*, 186−191.

(23) Sun, Z.; Feng, T.; Russell, T. P. Assembly of Graphene Oxide at Water/oil Interfaces: Tessellated Nanotiles. *Langmuir* **2013**, *29*, 13407−13413.

(24) Costa, L.; Li-Destri, G.; Thomson, N. H.; Konovalov, O.; Pontoni, D. Real Space Imaging of Nanoparticle Assembly at Liquid−Liquid Interfaces with Nanoscale Resolution. *Nano Lett.* **2016**, *16*, 5463−5468.

(25) Costa, L.; Li-Destri, G.; Pontoni, D.; Konovalov, O.; Thomson, N. H. Liquid-Liquid Interfacial Imaging Using Atomic Force Microscopy. *Adv. Mater. Interfaces* **2017**, *4*, 1700203.